J. Fluid Mech. (2007), *vol.* 574, *pp.* 393–403. © 2007 Cambridge University Press
doi:10.1017/S0022112006004198 Printed in the United Kingdom

A note on the propagation speed of a weakly dissipative gravity current

EUGENY V. ERMANYUK AND NIKOLAI V. GAVRILOV

Lavrentyev Institute of Hydrodynamics, 630090, Novosibirsk, Russia
ermanyuk@hydro.nsc.ru

(Received 4 October 2005 and in revised form 14 September 2006)

This paper presents an experimental study on the propagation speed of gravity currents at moderate values of a gravity Reynolds number. Two cases are considered: gravity currents propagating along a rigid boundary and intrusive gravity currents. For the first case, a semi-empirical formula for the front propagation speed derived from simple energy arguments is shown to capture well the effect of flow deceleration because of viscous dissipation. In the second case, the propagation speed is shown to agree with the one predicted for energy-conserving virtually inviscid flows (Shin, Dalziel & Linden, *J. Fluid Mech.* vol. 521, 2004, p. 1), which implies that the losses due to vorticity generation and mixing at the liquid–liquid interface play only a minor role in the total balance of energy.

1. Introduction

Gravity currents, i.e. flows of fluid of one density propagating into a fluid of another density along a horizontal boundary, occur in many geophysical and industrial applications (see e.g. Simpson 1997). Depending on the physical properties of the fluids, the gravity currents may range from virtually inviscid flows (Benjamin 1968; Shin, Dalziel & Linden 2004) to essentially viscous ones (Hoult 1972; Huppert 1982). In the present paper we focus our attention on so-called lock-exchange flows. Such flows are generated experimentally in a rectangular channel by removing a partition that initially separates two fluids of equal depth and different density, say salt and fresh water. In a more refined statement of the problem, a heavy fluid occupies only a fraction of full depth, while the upper layer of fluid has the same density as the homogeneous fluid on the other side of the partition. The two statements of the problem are known as full- and partial-depth releases. The history of the problem has been described in Shin *et al.* (2004) and Lowe, Rottman & Linden (2005) in great detail.

It is known that after the removal of the partition, during the slumping phase the front of the gravity current (see Rottman & Simpson 1983) moves at constant speed, which can be evaluated analytically using the model of an ideal fluid. The front speed in the case of the full-depth release is consistent with Benjamin's (1968) energy-conserving solution. In the case of the partial-depth release, the flows considered by Benjamin (1968) are not energy-conserving. An energy-conserving solution for the partial-depth release has recently been found and supported by a representative body of experimental data in Shin *et al.* (2004). The solution given in Shin *et al.* (2004) is valid only at sufficiently large values of the Reynolds number.

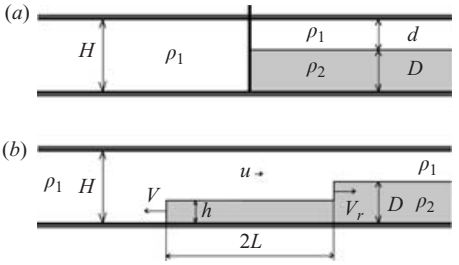

FIGURE 1. A sketch of a lock-exchange flow (*a*) before and (*b*) after release.

However, the range of applicability of energy-conserving arguments to real gravity flows with viscous dissipation has not been studied systematically. This problem is addressed in the present paper, where we suggest a simple semi-empirical formula for the propagation speed of a weakly dissipative gravity current, which takes into account the energy losses. The empirical coefficient of energy losses is evaluated from a series of experiments conducted in a range of the gravity Reynolds number $Re = (g'H^3/\nu^2)^{1/2}$ from 1600 to 28 000 (here H is the channel depth, ν is the reference kinematic viscosity, $g' = g(\rho_2 - \rho_1)/\rho_1$ is the reduced gravity acceleration, ρ_2 and ρ_1 are the densities of the heavy and light fluids, respectively). The results of experiments with the gravity currents propagating along a rigid boundary are compared with the results of a complementary set of experiments with intrusive gravity flows that can be considered as gravity flows propagating along a free-slip boundary coupled with their mirror reflection at this boundary. The comparison suggests that the energy losses due to mixing and shear at the liquid–liquid interface in the range of parameters covered play only a minor role in the total energy balance.

Section 2 of this paper presents a brief theoretical summary. A description of the experimental installation and techniques is given in § 3. The results of experiments with gravity currents and intrusive flows are described in § 4. A brief summary is presented in § 5.

2. Theoretical framework

Let us consider the flow scheme depicted in figure 1, where (*a*) and (*b*) sketches show the initial state of the system and a released gravity current, respectively. Initially, a thin partition separates a homogeneous fluid of density ρ_1 and a two-fluid system with the lower layer of density ρ_2 and depth D and the upper layer of density ρ_1 and depth d. The total depth H is the same on both sides from the partition so that $(d + D) = H$. The fluid is assumed to be bounded by two smooth rigid horizontal boundaries. Once the partition is removed, the front of the gravity current moves with the speed V and a rarefaction wave propagates in the opposite direction with speed V_r. Shin *et al.* (2004) have suggested a model for the flow depicted in figure 1. They assume that the fluid is inviscid and immiscible, and the flow is irrotational in each layer. The shape of the interface is taken to be horizontal, with two advancing fronts moving at constant speed. Away from the fronts the flow is assumed to be horizontal, with hydrostatic pressure gradient. Applying mass, momentum and energy conservation, Shin *et al.* (2004) show that: (i) all particles of the lower fluid between the front and the backward disturbance move with speed V and the particles of the upper fluid move with speed $u = Vh/(H - h)$, (ii) the depth of the gravity current after release is one-half of the initial depth, i.e. $h = D/2$, (iii) the speed of the backward

disturbance (a rarefaction wave) V_r is equal to the current front speed V. Accordingly, the rates of change of kinetic and potential energy of the system are

$$\dot{T} = \rho_2 V^3 h + \rho_1 V^3 h^2/(H-h), \tag{2.1}$$

$$\dot{P} = (\rho_2 - \rho_1) g V h^2, \tag{2.2}$$

where g is the gravity acceleration. Taking the reference density ρ so that $\rho \approx \rho_2 \approx \rho_1$ and introducing the relative density difference ε as $\varepsilon \approx (\rho_2 - \rho_1)/\rho$, substitution of (2.1) and (2.2) into the energy balance equation

$$\dot{T} = \dot{P} \tag{2.3}$$

yields the following formula for the gravity-current propagation speed:

$$Fr(\alpha) = (1-\alpha)^{1/2}, \tag{2.4}$$

where $\alpha = h/H$ is the fractional depth of the gravity current and the Froude number is defined as $Fr = V(g'h)^{-1/2}$, with $g' = \varepsilon g$. Note that (2.4) derived in Shin *et al.* (2004) for energy-conserving flows differs significantly from the formula given by Benjamin (1968):

$$Fr(\alpha) = \left[\frac{(1-\alpha)(2-\alpha)}{1+\alpha}\right]^{1/2}. \tag{2.5}$$

Formulas (2.4) and (2.5) yield the same result at $\alpha = 0.5$ when Benjamin's flows are energy-conserving. As $\alpha \to 0$, (2.4) and (2.5) predict values of the Froude number that are different by the factor of $2^{1/2}$. The experimental data obtained in Shin *et al.* (2004) strongly support formula (2.4) for energy-conserving flows. In the case of gravity currents with dissipation (2.4) is only valid at sufficiently large values of Reynolds number.

As will be discussed in § 3, experimental observations show that because of viscous losses the propagation speed of the gravity current measured at a certain distance from the lock gate is appreciably smaller than that predicted by (2.4). Note that this effect is different from the flow deceleration scenario in the case of finite lock length (see Huppert & Simpson 1980; Rottman & Simpson 1983; and a recent analysis, discussion and review of the history of the problem are given in Marino, Thomas & Linden 2005).

To take into account the loss of kinetic energy due to viscous friction we should introduce an additional term into the energy balance equation (2.3) as follows:

$$\dot{T} + \dot{E}_d = \dot{P}, \tag{2.6}$$

where $\dot{E}_d$ is the rate of the energy dissipation. The dissipated power can be evaluated by integrating a dissipation function e_d over the volume of the gravity current. An evaluation of the energy dissipation in a viscous shear flow can be found in any textbook on hydrodynamics (e.g. Batchelor 1967; Landau & Lifshitz 1987). According to the scheme depicted in figure 1, the flows of the upper and lower fluids are essentially horizontal. The dissipation function can be taken in the form $e_d = \mu(\mathrm{d}U/\mathrm{d}y)^2$, where $U(y)$ is the velocity distribution over the vertical coordinate, and $\mu = \rho\nu$ is the dynamic viscosity. Further, we assume that the vertical scales of the shear layers in the upper and lower fluids are proportional to $H-h$ and h, respectively. Correspondingly, the characteristic scales of $\mathrm{d}U/\mathrm{d}y$ in the upper and lower fluids are proportional to $u/(H-h)$ and V/h. Under these assumptions, the

total rate of energy dissipation in a current of total length $2L$ can be estimated as

$$\dot{E}_d = 2C_2\rho_2\nu_2\left(\frac{V}{h}\right)^2 hL + 2C_1\rho_1\nu_1\left(\frac{Vh}{(H-h)^2}\right)^2 (H-h)L$$

where C_1 and C_2 are empirical coefficients. Assuming for simplicity that $C_1 \approx C_2 \approx C$ and $\nu_1 \approx \nu_2 \approx \nu$, we obtain

$$\dot{E}_d = C\rho\nu V^2 \frac{2\xi}{\alpha}\left[1 + \left(\frac{\alpha}{1-\alpha}\right)^3\right], \tag{2.7}$$

where $\xi = L/H$ is the non-dimensional distance between the current front and the position of the lock gate. Note that the second term in the square brackets in (2.7) reflects the relative contribution of the upper layer to the total energy losses. At low values of the fractional current depth α the quantity $(\alpha/(1-\alpha))^3$ is small compared to unity and the energy dissipation in the upper fluid may be safely neglected. Substituting (2.1), (2.2) and (2.7) into (2.6), we obtain a quadratic equation for the Froude number. The positive root of this equation yields the dependence of the Froude number on the fractional depth α, non-dimensional distance ξ and the gravity Reynolds number $Re = (g'H^3/\nu^2)^{1/2}$:

$$Fr(\alpha, \xi, Re) = \left[\left(\frac{C\xi}{Re}\varphi(\alpha)\right)^2 + (1-\alpha)\right]^{1/2} - \frac{C\xi}{Re}\varphi(\alpha), \tag{2.8}$$

with

$$\varphi(\alpha) = \frac{1-\alpha}{\alpha^{5/2}}\left[1 + \left(\frac{\alpha}{1-\alpha}\right)^3\right].$$

As $Re \to \infty$, expression (2.8) approaches the limit for the effectively inviscid fluid (2.4). However, at finite Re and ξ under the condition $\alpha^{5/2} \ll (C\xi/Re)$ formula (2.8) predicts the asymptotic behaviour of the Froude number at low α in the form $Fr \sim \alpha^{5/2}Re/(2C\xi)$. Therefore, the value of the Froude number at low α in a real viscous fluid may significantly differ from the value predicted by (2.4). It should be emphasized that expression (2.8) is obtained using a quasi-steady approach. This implies that the steady-state analysis of mass and momentum conservation given in Shin *et al.* (2004) for gravity flows with constant propagation speed is approximately valid at each time instant for a weakly dissipative case, and the dissipated power $\dot{E}_d$ in (2.6) is a sufficiently small quantity. If the quasi-steady approach is valid, the energy loss coefficient C should not be sensitive to the variation of the current length ξ. The dependence of empirical coefficient C on the governing parameters of the problem is evaluated in § 4 (from experimental data).

In the above considerations we have introduced a bulk measure for the energy dissipation and estimated it by an order-of-magnitude approach. However, the total energy dissipation may be attributed both to the vorticity generation at the interface between the upper and lower fluids and to the friction at the rigid boundaries. To identify the governing mechanism of the energy dissipation, we have performed a series of experiments with intrusive gravity currents. The geometrical set-up of these experiments is sketched in figure 2. The test tank is divided by a thin partition into two parts. One part is filled with a two-fluid system. The density of the upper and lower fluids is ρ_1 and ρ_3, respectively. The depth of each layer is H. The other part of the test tank is filled with three layers of fluid with densities ρ_1, ρ_2 and ρ_3. The upper and the lower layers are of equal depth $H - D$ and the middle layer has depth

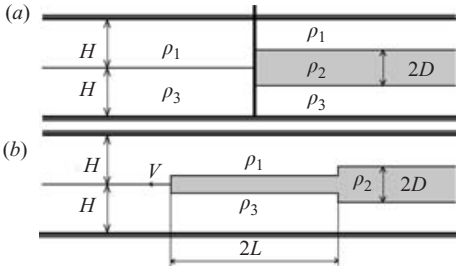

FIGURE 2. A sketch of an intrusive flow (*a*) before and (*b*) after release.

$2D$. The fluid densities satisfy the condition $\rho_2 - \rho_1 = \rho_3 - \rho_2$. Thus, one can consider the set-up shown in figure 2 as the gravity flow shown in figure 1 coupled with its mirror reflection with respect to the interface between the fluids with densities ρ_1 and ρ_3. Accordingly, the energy losses in the intrusive gravity current can be attributed entirely to vorticity generation and mixing at the liquid–liquid interface. It should be noted that some experimental data on intrusive flows depicted in figure 2 have been obtained in Britter & Simpson (1981). However, the data are difficult to interpret within the framework of the present study since the definition of the Froude number in Britter & Simpson (1981) involves a subjectively chosen vertical size of the current that is not related to the initial geometrical parameters of the problem. A study on the structure of the velocity field in an intrusive gravity current is presented in Lowe, Linden & Rottman (2002). More details on the dynamics of intrusive gravity currents with a more general relation between $(\rho_3 - \rho_2)$ and $(\rho_2 - \rho_1)$ are given in Rooij, Linden & Dalziel (1999), Sutherland, Kyba & Flynn (2004) and Cheong, Kuenen & Linden (2006).

3. Experimental set-up

Experiments were carried out in a test tank of length 320 cm, width 20 cm and depth 35 cm. The walls of the test tank were made of Perspex. The test tank was divided by a vertical slide gate in two equal parts. The geometrical set-up of the experiments is clear from the sketches shown in figures 1 and 2. A weak solution of sugar in water was used to create the stratification. Layered stratification was produced by filling one fluid above the other using a porous float. In a local coordinate system with the origin taken at the middle of an interface and the η-axis directed vertically upwards the measured density distribution over depth fitted the following approximation:

$$\rho(\eta) = \frac{1}{2}(\rho_- + \rho_+) - \frac{\rho_- - \rho_+}{2} \tanh\left(\frac{2\eta}{\delta}\right),$$

where δ is the characteristic thickness of the pycnocline, and ρ_+ and ρ_- are the asymptotic values of fluid densities of the upper and lower fluids, respectively. The density distribution was measured by a conductivity probe. All experiments were performed with a freshly prepared layered stratification. The value of δ in experiments did not exceed 1 cm.

Typically, a series of experiments was executed by keeping Re constant and performing several runs at different values of the fractional depth α. In the presentation of experimental data, the fractional depth and the Froude number are defined as $\alpha = D/2H$ and $Fr = V/(\frac{1}{2}\varepsilon g D)^{1/2}$, respectively. The front propagation speed was evaluated from video-records obtained by a digital camera at the acquisition rate of 25 frames per second. The visualization was performed by capturing the image

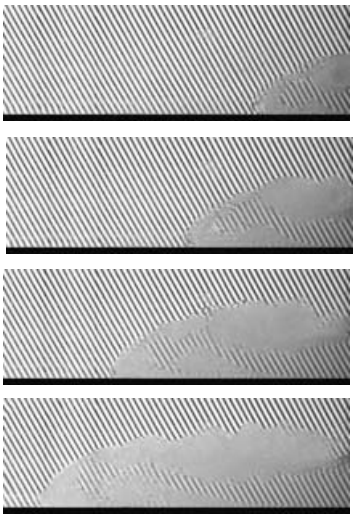

FIGURE 3. Development of the gravity current structure after a release: $\alpha = 0.4$, $H = 10\,\text{cm}$, $\varepsilon = 0.01$, the time-span between the successive frames is 1.27 s; the right edge of the frames is the 5 cm from the lock gate, the horizontal size of the frames is 20 cm.

of an illuminated pattern of inclined black and white stripes through the bulk of fluid. The camera was placed 2.5 m from the test tank. This method of visualization effectively reveals the qualitative features of the flow structure.

The value of the gravity Reynolds number $Re = (\varepsilon g H^3/\nu^2)^{1/2}$ in experiments could be varied by changing $\varepsilon = (\rho_2 - \rho_1)/\rho_1$ and/or H. The kinematic viscosity of the fluid with density ρ_2 was used as the reference value of ν. The main body of data was obtained at $H = 10\,\text{cm}$. In experiments with the set-up shown in figure 1 we have performed series of experiments at $H = 6$, 15, 20 and 30 cm. The relative density difference ε ranged from 0.0005 to 0.01 for the set-up shown in figure 1 and from 0.0007 to 0.01 for the set-up shown in figure 2. The range of gravity Reynolds numbers covered was from 1600 to 28 000 for gravity currents (figure 1) and from 2600 to 7000 for intrusive gravity currents (figure 2). The main motivation for experiments with intrusive gravity currents was to demonstrate the low energy losses compared to the case of gravity currents propagating along a rigid boundary. Hence, the parameter range in experiments with intrusive currents was reduced to a sufficiently representative minimum in view of the increased difficulties with the creation of initial stratification.

The weak sugar–water solutions having prescribed densities were prepared by mixing a carefully measured volume of a solution with density, say, $\rho_{ini} = 1.05\,\text{g cm}^{-3}$ with a known volume of fresh water. The density ρ_{ini} was measured with a standard hydrometer with accuracy $\pm 0.0005\,\text{g cm}^{-3}$. Taking into account a possible uncertainty in the volumes of the mixed fluids, the prescribed value of ε was maintained in experiments with accuracy $\pm 5\,\%$. Special care was taken to keep the prepared fluids of different densities at constant temperature to avoid any temperature difference that could affect the experimental results at low values of ε.

4. Results and discussion

The development of a gravity current after the removal of the partition in the case shown in figure 1 is illustrated in figure 3. One can identify the core region

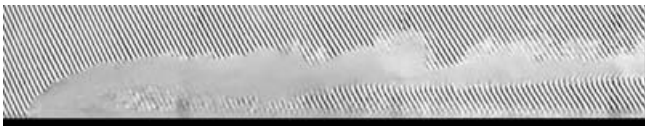

FIGURE 4. The structure of a fully developed gravity current: the head of the current is at distance $\xi = 8$ from the lock gate; experimental conditions are the same as in figure 3.

of the gravity current, which can be considered as quasi-homogeneous, and regions of intensive stirring developing at the interface between the upper and lower fluids. With the passage of time, the regions of intensive stirring tend to increase and merge. The flow structure of a fully developed gravity current is shown in figure 4. In § 2, it is assumed that the vertically integrated dissipation rate has the order of magnitude $C\rho\nu V^2[1 + \alpha^3/(1-\alpha)^3]/(\alpha H)$, being uniformly distributed between the fronts of the buoyant and dense fluids. The flow structure shown in figure 4 suggests that the vertically integrated dissipation rate varies along the current. A higher dissipation rate may be expected in the head part of the flow. Also, as the flow develops, one may expect some fluctuations of local dissipation rate associated with the regions of intensive stirring which are clearly seen in figure 3. Such a realistic distribution of a vertically integrated dissipation rate along the current is shown in figure 9 of Birman, Martin & Meiburg (2005), presenting the results of high-resolution numerical simulations. It should be kept in mind however that in the non-Boussinesq case considered in Birman *et al.* (2005) the behaviour of the buoyant fronts is qualitatively similar to the Boussinesq case considered in the present paper (see also discussion in Lowe *et al.* (2005). In principle, one can roughly decompose the distribution of the dissipation rate along the current into the sum of a uniform distribution and a fluctuating component. We assume that the uniform distribution of the dissipation rate along the current represents an order-of-magnitude measure for evaluation of the overall energy budget in our case. The time histories of the overall dissipated energy calculated in Birman *et al.* (2005) seem to be qualitatively consistent with our simplistic analysis. Unfortunately, a direct comparison is impossible since their study is focused on the non-Boussinesq case of the full-depth release ($\alpha = 0.5$), with the Schmidt number Sc (the ratio of kinematic viscosity to molecular diffusivity) equal to 1. In the case of a sugar-stratified fluid we have $Sc \approx 2500$.

Experimental dependence of the Froude number Fr on the fractional depth α measured at different values of Re and fixed $\xi = 4$ is shown in figure 5 for the gravity currents propagating along a rigid horizontal bottom (i.e. for the set-up sketched in figure 1). Benjamin's (1968) solution (2.5) and the solution (2.4) obtained in Shin *et al.* (2004) for the energy-conserving flows are shown by lines 1 and 2, respectively. Curves 3 to 7 show the least-squares approximations of the experimental data using expression (2.8). At sufficiently large α and Re, the experimental data and their approximations are close to line 2 predicted by (2.4) for ideal fluids. As Re and α decrease, viscous dissipation becomes increasingly important, leading to a significant departure of experimental data from line 2. One can see that (2.8) captures this effect well. The dependence of the energy loss coefficient C on Re resulting from the least-squares fit of experimental data using expression (2.8) is shown in figure 6. The typical scatter of data around the approximating curves (2.8) in figure 5 corresponds to the scatter of C of about $\pm 20\,\%$ of the value evaluated from the least-squares fit. The squares in figure 6 show the estimated values of C corresponding to the data from figure 5. About 50 experimental runs at seven additional values of the Reynolds number (roughly seven runs at different values of α per value of the Reynolds number)

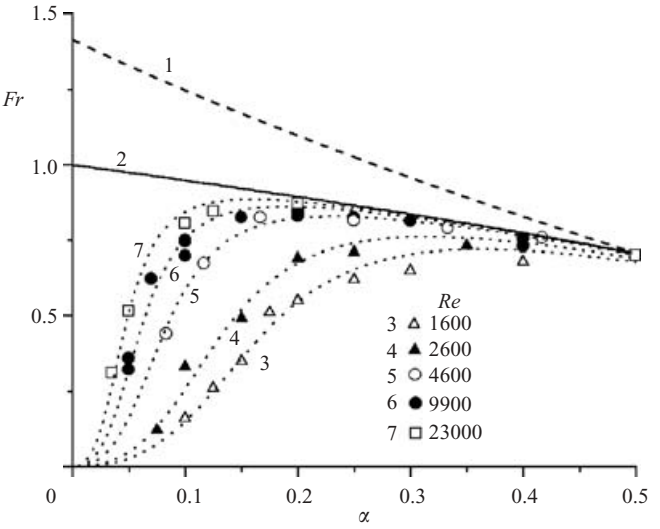

FIGURE 5. Froude number of the gravity current Fr vs. fractional depth α for different values of the gravity Reynolds number Re; lines 1 and 2 correspond to Benjamin's (1968) theory and solution (2.4) for energy-conserving flows (Shin *et al.* 2004), respectively; symbols and lines 3 to 7 represent experimental data and their least-squares approximations using formula (2.8).

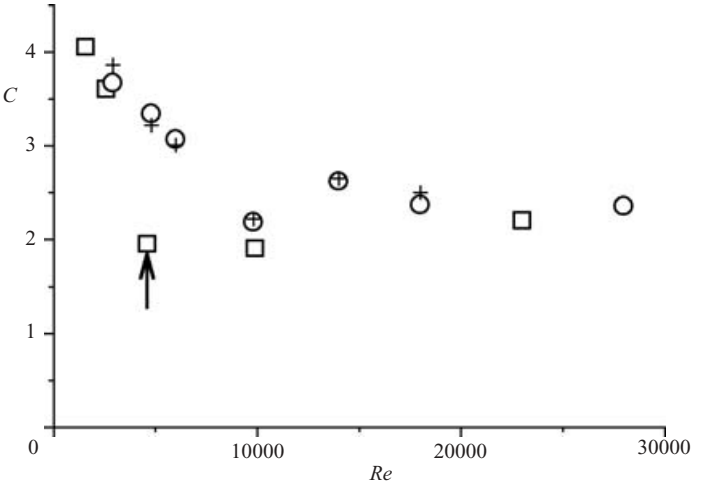

FIGURE 6. Experimental values of the energy loss coefficient C at different values of the gravity Reynolds number Re: squares correspond to the data from figure 4, circles and crosses correspond to the data obtained in additional series of experiments at $\xi = 4$ and $\xi = 8$, respectively; the arrow shows the point obtained at $H = 6$ cm, all the other points were obtained at H between 10 cm and 30 cm.

were executed to provide a sufficiently representative body of data on the values of C at different Re. The measurements in each run were taken at $\xi = 4$ and $\xi = 8$, shown in figure 6 by circles and crosses, respectively. The good agreement between the values of C at $\xi = 4$ and $\xi = 8$ provides support for the quasi-steady approach used in the derivation of (2.8). In the range $1600 \leqslant Re \leqslant 6000$ the loss coefficient C gradually decreases with Re. We have not observed any abrupt change of the flow regime with Re in the range of parameters studied. The variation of C with Re is presumably caused by the gradual change of the velocity distribution over vertical coordinate

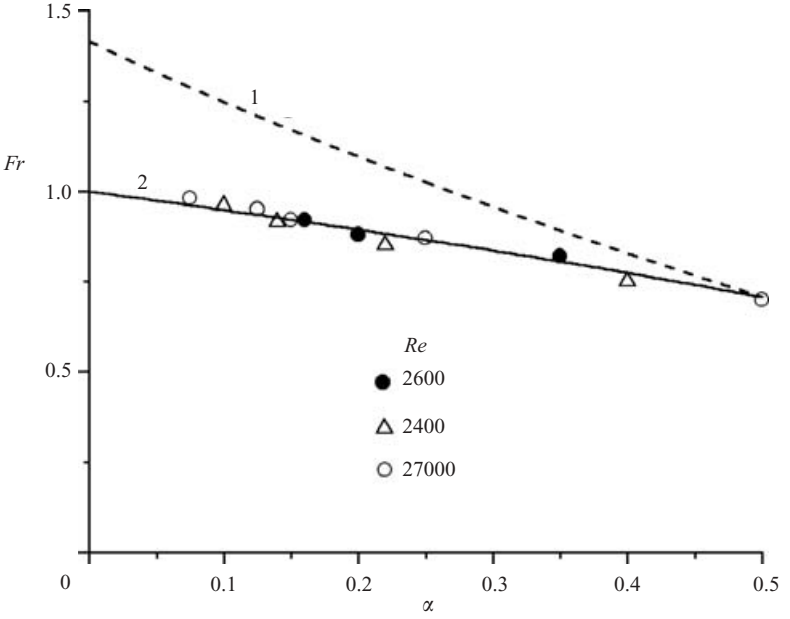

FIGURE 7. Froude number of the intrusive gravity current Fr vs. fractional depth α for different values of the gravity Reynolds number Re; lines 1 and 2 correspond to Benjamin's (1968) theory and to the solution (2.4) for energy-conserving flows (Shin *et al.* 2004), respectively.

$U(y)$ with Re. When $Re > 6000$ coefficient C remains constant up to $Re = 28\,000$, the highest value in the present experiments. In this range the mean estimated value of the loss coefficient is $C \approx 2.4$.

The point marked in figure 6 by the arrow seems to fall outside the general dependence. This point corresponds to the data obtained at $H = 6$ cm, the lowest value of the channel depth in the present experiments. Correspondingly, one can expect, first, lower accuracy in evaluation of α, and, second, a greater impact of finite pycnocline thickness on the results of the experiments; the pycnocline thickness δ varied little throughout the experimental runs. The quantities δ/H and $\delta/D = \delta/(2\alpha H)$ can be introduced to characterize the departure of the experimental stratification from an idealized two-layer case. It should be kept in mind that the effect of a finite pycnocline thickness could have some influence on the data obtained at low α. However, for the data obtained at H between 10 cm and 30 cm the values of the energy loss coefficient C shown in figure 6 have not demonstrated any detectable trend that could be attributed to the effect of finite δ.

Expression (2.8) and the data presented in figure 6 give us a tool for quantitative evaluation of effects due to the finite values of Re and α. In the experiments described in Shin *et al.* (2004) the lowest values of α were about 0.05 at $Re \sim 270\,000$ and $\xi \simeq 2$. Assuming $C \approx 2.4$, we can estimate that the difference between the values of the Froude number predicted by (2.8) and (2.4) under the above conditions is about 3 % so that the gravity currents considered in Shin *et al.* (2004) were indeed effectively inviscid.

The results of experiments with intrusive gravity currents are presented in figure 7. One can see that the experimental points obtained at Re between 2600 and 7000 fall on the theoretical curve (2.4) corresponding to inviscid energy-conserving flows. The front of the intrusive current in the range of experimental conditions considered has not shown any tendency to decelerate with distance. Such a behaviour indicates that

the energy losses at the liquid–liquid interface are small. Note that it is difficult to decrease Re and α beyond the values attained in the present experiments. On the one hand, it is complicated to work with a layered stratification at a density difference ε below 0.0005 and on the other hand the ratio δ/D must be sufficiently small (the effect of the latter parameter on the propagation speed of an intrusive gravity current has been described in Britter & Simpson 1981).

5. Conclusion

In this work we have made an attempt to estimate quantitatively the energy losses in a weakly dissipative gravity current propagating along a rigid horizontal boundary. It is assumed that at a first approximation, the properties of the current are consistent with the solution given in Shin *et al.* (2004) for energy-conserving virtually inviscid gravity currents. Then, a dissipative term is added to the energy balance equation. The rate of energy dissipation is estimated by an order-of-magnitude approach. The resulting semi-empirical formula for the gravity current propagation speed is found to capture the experimentally observed deceleration of the gravity currents at finite values of the gravity Reynolds number. An additional set of experiments with intrusive gravity currents (which can be interpreted as gravity currents propagating along a free-slip boundary) has demonstrated that their front speed is consistent with that for energy-conserving gravity flows (Shin *et al.* 2004) and the effects of finite gravity Reynolds number are small in the considered range of experimental parameters. In general, the present results suggest that in terms of the total energy balance the energy losses due to vorticity generation and mixing at the interface between the gravity current and the ambient fluid are far less important than the losses due to bottom friction.

It should be mentioned that the present experiments have been conducted in the parameter range where the dissipative effects are most pronounced at low values of the fractional depth, being related to the shear in the heavier fluid. Consequently, we cannot draw a firm conclusion concerning the assumptions about the bulk measure for shear and dissipation in the light fluid.

In the theoretical framework of the present paper we assume that the dissipation is weak so that a quasi-steady approach can be used for evaluation of the overall energy balance. These assumptions are found to be consistent with the experimental data in the parameter range studied. However, the applicability of such approach to a general case of decelerating flows with dissipation remains an open issue.

The authors are grateful to the referees for their constructive comments. Thanks are due to Professor N. I. Makarenko for interesting discussions. This study was partially supported by the Russian Foundation for Basic Research under grant No. 04-01-00040 and by the Russian Academy of Sciences under grant No. 4.13.1.

REFERENCES

Batchelor, G. K. 1967 *An Introduction to Fluid Dynamics*. Cambridge University Press.

Benjamin, T. B. 1968 Gravity currents and related phenomena. *J. Fluid Mech.* **31**, 209–248.

Birman, V. K., Martin, J. E. & Meiburg, E. 2005 The non-Boussinesq lock-exchange problem. Part 2. High-resolution simulations. *J. Fluid Mech.* **537**, 125–144.

Britter, R. E. & Simpson, J. E. 1981 A note on the structure of the head of an intrusive gravity current. *J. Fluid Mech.* **112**, 459–466.

Cheong, H.-B., Kuenen, J. J. P. & Linden, P. F. 2006 The front speed of intrusive gravity currents. *J. Fluid Mech.* **552**, 1–11.

Hoult, D. P. 1972 Oil spreading on the sea. *Annu. Rev. Fluid Mech.* **4**, 341–368.

Huppert, H. E. 1982 The propagation of two-dimensional and axisymmetric viscous gravity currents over a rigid horizontal surface. *J. Fluid Mech.* **121**, 43–58.

Huppert, H. E. & Simpson, J. E. 1980 The slumping of gravity currents. *J. Fluid Mech.* **99**, 785–799.

Landau, L. D. & Lifshitz, E. M. 1987 *Fluid Mechanics*. Butterworth-Heineman.

Lowe, R. J., Linden, P. F. & Rottman, J. W. 2002 A laboratory study of the velocity structure in an intrusive gravity current. *J. Fluid Mech.* **456**, 33–48.

Lowe, R. J., Rottman, J. W. & Linden, P. F. 2005 The non-Boussinesq lock-exchange problem. Part 1. Theory and experiments. *J. Fluid Mech.* **537**, 101–124.

Marino, B. M., Thomas, L. P. & Linden, P. F. 2005 The front condition for gravity currents. *J. Fluid Mech.* **536**, 49–78.

Rooij, F., Linden, P. F. & Dalziel, S. B. 1999 Saline- and particle-driven interfacial intrusions. *J. Fluid Mech.* **389**, 303–334.

Rottman, J. W. & Simpson, J. E. 1983 Gravity currents produced by instantaneous releases of a heavy fluid in a rectangular channel. *J. Fluid Mech.* **135**, 95–110.

Shin, J. O., Dalziel, S. B. & Linden, P. F. 2004 Gravity currents produced by lock exchange. *J. Fluid Mech.* **521**, 1–34.

Simpson, J. S. 1997 *Gravity Currents: In the Environment and the Laboratory*, 2nd Edn. Cambridge University Press.

Sutherland, B. R., Kyba, P. J. & Flynn, M. R. 2004 Intrusive gravity currents in two-layer fluids. *J. Fluid Mech.* **514**, 327–353.